

# EPR Evidence for hydroxyl- and substrate-derived radicals in Fe(II)-oxalate/hydrogen peroxide reactions. The importance of the reduction of Fe(III)-oxalate by oxygen-conjugated radicals to regenerate Fe(II) in reactions of carbohydrates and model compounds

Jonathan S. B. Park,<sup>a</sup> Paul M. Wood,<sup>a</sup> Bruce C. Gilbert<sup>\*b</sup> and Adrian C. Whitwood<sup>b</sup>

<sup>a</sup> Department of Biochemistry, University of Bristol, School of Medical Sciences, University Walk, Bristol, UK BS8 1TD

<sup>b</sup> Department of Chemistry, University of York, Heslington, York, UK YO10 5DD

Received (in Cambridge) 2nd February 1999, Accepted 19th March 1999

EPR spectroscopy has been employed for the direct detection of a variety of free radicals formed from reaction of Fe(II)-oxalate and H<sub>2</sub>O<sub>2</sub> in the presence of carbohydrates and related compounds: this system has been designed to model the proposed mode of action of brown rot fungi. The observed hyperfine splittings allow characterization of individual radicals formed at different positions in the carbohydrate rings. Relative signal intensities in steady-state spectra indicate the rapid generation of the hydroxyl radical, followed by relatively unselective attack of  $\cdot\text{OH}$  on the substrates' C-H bonds: the rapidity of oxidation by Fe(III) of oxygen-conjugated carbon-centred radicals (typically  $k$  10<sup>8</sup> dm<sup>3</sup> mol<sup>-1</sup> s<sup>-1</sup>) is significantly reduced if there is an eclipsing  $\beta$ -oxygen substituent. The relevance of these findings to cellulose-cleaving reactions of certain fungi is discussed.

## Introduction

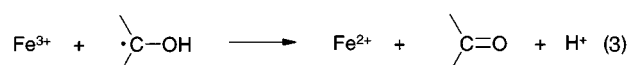
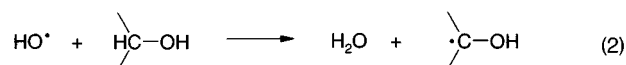
The growth of certain timber-decaying fungi has serious implications for load-bearing structures at a relatively early stage of attack. These fungi belong to a physiological class known as brown rot, which includes dry rot (*Serpula lacrymans*) and cellar rot (*Coniophora puteana*). Their attack causes loss of strength because cleavage of the long glucose chains in cellulose takes place not only close to the hyphae but also within the wood cell wall and in adjacent cells.<sup>1</sup> Evidence has built up for hydroxyl radicals (HO $\cdot$ ) as the causative agent:<sup>2</sup> as in many biological systems, the source of HO $\cdot$  is believed to be the reaction of Fe(II) with H<sub>2</sub>O<sub>2</sub> [reaction (1)]. A further characteristic of these fungi is the secretion of oxalic acid<sup>3</sup> and in our earlier kinetic study of the reaction of H<sub>2</sub>O<sub>2</sub> with Fe(II)-oxalate complexes, rate constants were measured that are faster than for most Fe(II) chelates.<sup>4</sup>

It is notable that brown rot fungi tend to cleave cellulose at regions of slight disorder, leaving microcrystallites as opposed to smaller fragments.<sup>5</sup> This implies that production of HO $\cdot$  occurs at specific sites, rather than as a random event. The data presented below provide further evidence for generation of  $\cdot\text{OH}$  from Fe(II)-oxalate and H<sub>2</sub>O<sub>2</sub> and for regeneration of Fe(II) by reaction of oxygen-conjugated radicals with Fe(III)-oxalate [reactions (2) and (3)]. If the Fe is bound and H<sub>2</sub>O<sub>2</sub> is mobile, this recycling of Fe(II) provides a mechanism for multiple production of HO $\cdot$  at the same site.

From continuous-flow EPR studies with the Ti(III)/H<sub>2</sub>O<sub>2</sub> couple, for which a steady-state is believed to be achieved in the

cavity of the spectrometer, it is believed that reaction of HO $\cdot$  with ethanol leads to the formation of  $\alpha$ - and  $\beta$ -radicals ( $\cdot\text{CHMeOH}$  and  $\cdot\text{CH}_2\text{CH}_2\text{OH}$ , respectively) in the ratio 13:1;<sup>6</sup> by contrast, in similar experiments with Fe(II)-EDTA/H<sub>2</sub>O<sub>2</sub>, the ratio is typically less than 1:1.<sup>7</sup> On the basis of such differences, however, it has been suggested that the attacking species must be other than HO $\cdot$  [e.g. high valent iron: see discussion in ref. 7]. However, EPR studies of the Fe(II)-EDTA/H<sub>2</sub>O<sub>2</sub> system with a wide range of organic compounds have demonstrated that the radicals detected are qualitatively exactly as expected for attack by HO $\cdot$ :<sup>7</sup> the observed low  $\alpha$ :- $\beta$ - ratio for radicals from ethanol is explained in terms of secondary reactions, of which the most important is the extremely rapid reaction of the  $\alpha$ -radical with Fe(III)-EDTA (with  $k$  in the range 1.0–1.5  $\times$  10<sup>9</sup> M<sup>-1</sup> s<sup>-1</sup>)<sup>7</sup> cf. reaction (3) above. This rapid reaction, which is an example of Fe(II) regeneration as discussed above, reflects the effect of the electron-donating (+M) oxygen substituent on the radical centre and the resulting encouragement of electron transfer, with stabilization of the resulting incipient carbonium ion,  $\text{Me}\overset{\ominus}{\text{C}}\text{H}-\text{OR} \leftrightarrow \text{MeCH}=\overset{\oplus}{\text{C}}\text{R}$ .

In our earlier EPR and kinetic study of the reactions in Fe(II)/H<sub>2</sub>O<sub>2</sub> systems with oxalate as chelator, we showed that addition of *tert*-butyl alcohol gives rise to the detection of characteristic signals from  $\cdot\text{CH}_2\text{CMe}_2\text{OH}$ , as expected if HO $\cdot$  is the attacking species.<sup>4</sup> Our first objective in the work to be described here was to show that with ethanol as substrate, the ratio of  $\alpha$ :- $\beta$ - radicals is consistent with HO $\cdot$  formation and subsequent preferential reaction of the  $\alpha$ -radical with Fe(III)-oxalate, and to estimate a rate constant for this process. In view of our interest in cellulose breakdown, our next aim was to study the EPR spectra obtained from Fe(II)-oxalate/H<sub>2</sub>O<sub>2</sub> in the presence of carbohydrates such as D-glucose and some model compounds; such spectra have previously only been studied with Ti(III)/H<sub>2</sub>O<sub>2</sub> as the source of HO $\cdot$ .<sup>8–10</sup> As we shall show, the results obtained are apparently different from those reported for Ti(III)/H<sub>2</sub>O<sub>2</sub>, but can again be explained by selective removal of certain radicals (formed by the generation and reaction of  $\cdot\text{OH}$ ) by subsequent 1-electron transfer to Fe(III). Mechanistic



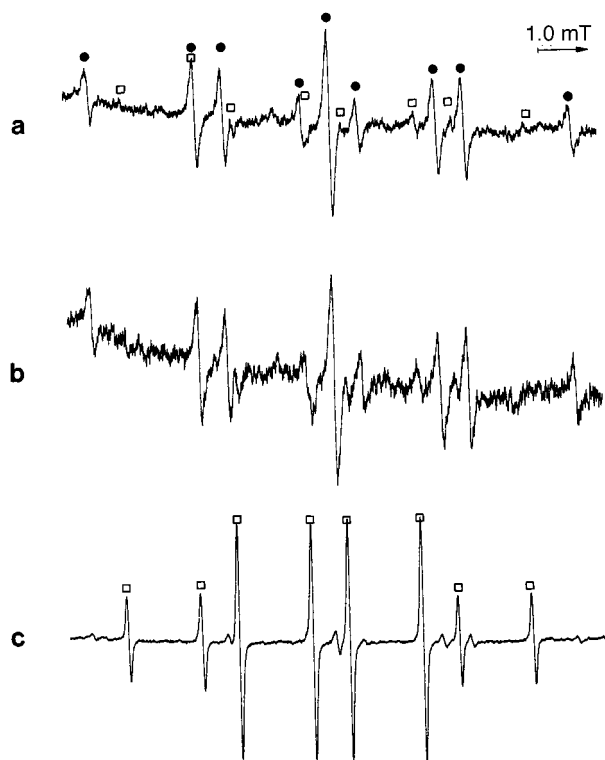


**Fig. 1** EPR spectra of  $\cdot\text{CH}_2\text{CH}_2\text{OH}$  (●) and  $\cdot\text{CH}(\text{CH}_3)\text{OH}$  (□) obtained from the reaction of ethanol (5% v/v), hydrogen peroxide (8 mM) and a solution of (a) Fe(II)-oxalate (2 mM); (b) Fe(II)-EDTA (2 mM); (c) Ti(III)-EDTA (2 mM).

and kinetic analysis is provided and the relevance to cellulose degradation discussed.

## Results

### 1. Fe(II)-oxalate/ $\text{H}_2\text{O}_2$ reactions in the presence of ethanol

**1.1 Initial EPR studies.** Fig. 1(a) shows the EPR spectrum obtained by rapid mixing of Fe(II)-oxalate with  $\text{H}_2\text{O}_2$  in the presence of ethanol in the cavity of the spectrometer (see Experimental section for further details); the two spectra in Fig. 1(b) and (c) were obtained under comparable conditions, but with Fe(II)-EDTA and Ti(III)-EDTA, respectively, instead of Fe(II)-oxalate. It can be readily seen that the steady-state spectrum observed with Ti(III)-EDTA is dominated by signals from the  $\alpha$ -radical, as explained above.<sup>7</sup> The spectrum with Fe(II)-oxalate is similar to that observed with Fe(II)-EDTA with both having a much reduced  $\alpha/\beta$  ratio: the  $\alpha/\beta$  ratio was estimated as 0.23 for Fe(II)-EDTA and 0.16 for Fe(II)-oxalate under our standard conditions (see Experimental section).

**1.2 Kinetic analysis.** We next followed the procedure described earlier in a kinetic investigation of the Fe(II)-EDTA/ $\text{H}_2\text{O}_2$  reaction in the presence of ethanol, which involved determination of the steady-state  $\alpha/\beta$  ratio as a function of both  $[\text{Fe(II)}]_0$  and  $[\text{H}_2\text{O}_2]_0$ .<sup>7</sup> The results are listed in Table 1; this illustrates the general trend of a reduction in  $\alpha/\beta$  ratio as either Fe(II) or  $\text{H}_2\text{O}_2$  is increased. This behaviour can be understood in terms of the enhanced rate of oxidation of  $\cdot\text{CHMeOH}$  by Fe(III) in the cavity; the flux through reaction (1) is faster leading to increased levels of Fe(III).<sup>7</sup>

Table 1 also shows the behaviour simulated for the  $\alpha/\beta$  ratio using the following reaction scheme [reactions (4)–(12)] and

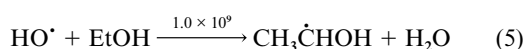
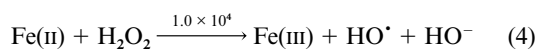
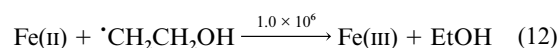
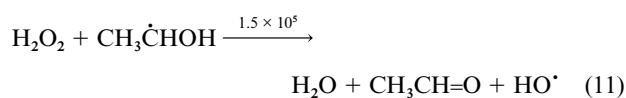
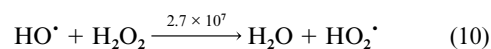
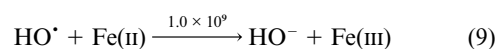
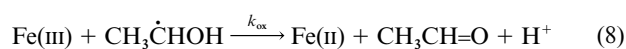
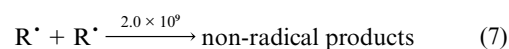
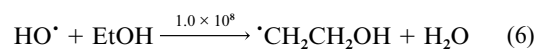


**Table 1** Experimental and simulated variation of the ratio of  $[\cdot\text{CHMeOH}]/[\cdot\text{CH}_2\text{CH}_2\text{OH}]$  ( $\alpha/\beta$ ) radicals with initial Fe(II) and  $\text{H}_2\text{O}_2$  concentrations

$[\text{Fe(II)}]_0/\text{mM}$	$[\text{H}_2\text{O}_2]_0/\text{mM}$	Experimental ( $\alpha/\beta$ ) <sup>a</sup>	Simulated ( $\alpha/\beta$ ) <sup>b</sup>
0.5	4.0	0.268	0.344
1.5	4.0	0.217	0.221
3.0	4.0	0.191	0.166
0.5	8.0	0.210	0.241
1.5	8.0	0.167	0.156
3.0	8.0	0.150	0.111

<sup>a</sup> Error estimated to be  $\pm 0.05$ . <sup>b</sup> Calculated values of absolute radical concentration were in good agreement with experimental values, e.g. with  $[\text{Fe(II)}]_0$  1.5 mM and  $[\text{H}_2\text{O}_2]_0$  4.0 mM,  $[\alpha]_{\text{expt}} = 0.187 \mu\text{M}$ ,  $[\beta]_{\text{expt}} = 0.861 \mu\text{M}$ ,  $[\alpha]_{\text{calc}} = 0.195 \mu\text{M}$ ,  $[\beta]_{\text{calc}} = 0.884 \mu\text{M}$ .



with different values for the rate constant for electron-transfer from  $\cdot\text{CHMeOH}$  [other rate constants are generally accepted values as used previously,<sup>7</sup> all rate constants are in  $\text{dm}^3 \text{mol}^{-1} \text{s}^{-1}$ ]. There was good agreement between experimental and calculated radical concentrations. The value obtained for  $k_{\text{ox}}$  is thus estimated as  $6 \times 10^8 \text{ dm}^3 \text{mol}^{-1} \text{s}^{-1}$  which can be compared with a value of  $k_{\text{ox}}$  of  $1\text{--}1.5 \times 10^9 \text{ dm}^3 \text{mol}^{-1} \text{s}^{-1}$  for the reaction between Fe(III)-EDTA and  $\cdot\text{CHMeOH}$ , again close to the diffusion-controlled limit. Note that the rate of oxidation of non-conjugated radicals is expected to be much lower and has not been included; we have included, however, a contribution for reduction of  $\cdot\text{CH}_2\text{CH}_2\text{OH}$  ( $k$   $1.0 \times 10^6 \text{ dm}^3 \text{mol}^{-1} \text{s}^{-1}$ ) by  $\text{Fe}^{\text{II}}$ , as described earlier [reaction (12)].<sup>4</sup>

### 2. Use of EPR spectroscopy to detect radicals from reaction of other model compounds with the Fe(II)-oxalate/ $\text{H}_2\text{O}_2$ redox couple

Related experiments were carried out with a variety of oxygen-containing substrates (with mono- or  $\alpha,\beta$ -difunctionality) to determine whether the interpretation given above is more widely applicable. Examples of the results are shown in Fig. 2, and hyperfine splittings of the radicals detected are listed in Table 2. Experiments were also carried out with each substrate using the Ti(III)/ $\text{H}_2\text{O}_2$  couple to ascertain the appropriate  $\alpha/\beta$  ratio which arises from  $\text{HO}\cdot$  attack in the absence of radical oxidation, *i.e.* which will indicate the different reactivities of the C–H bonds in the appropriate molecules towards  $\text{HO}\cdot$ .

The behaviour of diethyl ether resembles that of ethanol; the  $\beta$ -radical,  $\cdot\text{CH}_2\text{CH}_2\text{OEt}$  (**1**) is dominant, with only a trace of the  $\alpha$ -radical  $\cdot\text{CHMeOEt}$  (**2**) detectable. Similar behaviour was

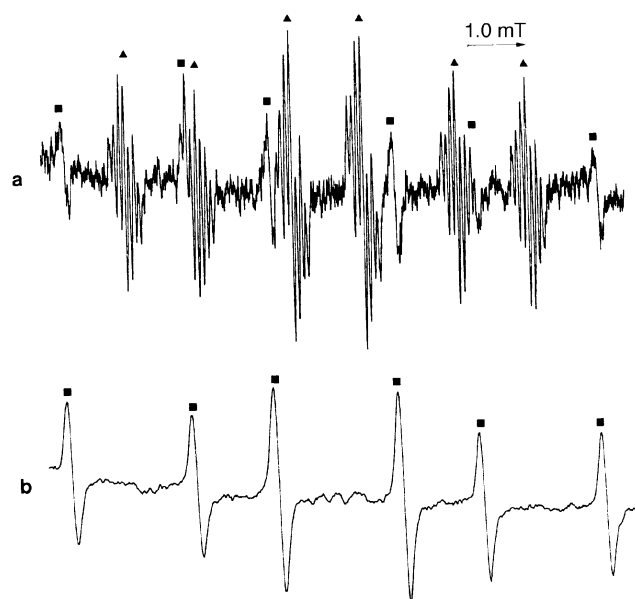


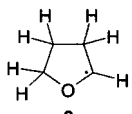
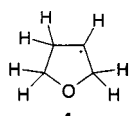
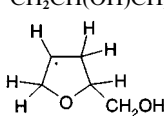
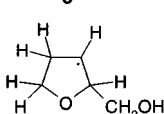
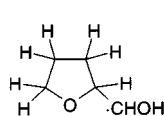
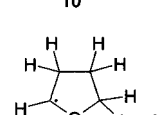
**Fig. 2** Central portion of the EPR spectra of radicals (3, ▲) and (4, ■) obtained from the reaction of tetrahydrofuran (50 mM), hydrogen peroxide (8 mM) and a solution of (a) Ti(III)-EDTA (2 mM); (b) Fe(II)-oxalate (2 mM).

observed for tetrahydrofuran for which, in contrast to the Ti(III)/H<sub>2</sub>O<sub>2</sub> system (for which both  $\alpha$ - and  $\beta$ -radicals 3 and 4 are detected, with  $[a] > [\beta]$ ), dominant signals for the non-conjugated  $\beta$ -radical were again observed (see Fig. 2). This is entirely consistent with the argument that the  $\alpha$ -radicals are destroyed by rapid reaction with Fe(III)-oxalate. For propane-1,2-diol, which gives strong signals from  $\cdot\text{CH}(\text{OH})\text{CHMeOH}$  (5),  $\cdot\text{CMe}(\text{OH})\text{CH}_2\text{OH}$  (6) and  $\cdot\text{CH}_2\text{CH}(\text{OH})\text{CH}_2\text{OH}$  (7) with Ti(III)/H<sub>2</sub>O<sub>2</sub> (at pH 4), only a signal from the non-conjugated radical 7 was observed with Fe(II)-oxalate/H<sub>2</sub>O<sub>2</sub>, as would be expected on the same basis. With tetrahydrofurfuryl alcohol the spectrum with the Fe(II)-oxalate system is dominated by signals from 8 and 9, whereas with Ti(III)/H<sub>2</sub>O<sub>2</sub> a complex spectrum is dominated by signals from the oxygen-conjugated radicals 10 and 11 with only traces of 8 and 9.

### 3. EPR Studies of the reaction of carbohydrates with the Fe(II)-oxalate/H<sub>2</sub>O<sub>2</sub> couple

**3.1  $\alpha$ -D-Glucose and  $\beta$ -D-glucose.** Fig. 3(a) shows the very well-resolved and complex spectrum obtained from reaction of  $\cdot\text{OH}$  [from Ti(III)-EDTA/H<sub>2</sub>O<sub>2</sub>] with  $\alpha$ -D-glucose in aqueous solution at pH 4.<sup>9</sup> all the spectra were recorded at this pH to avoid the occurrence of acid- or base-catalysed rearrangement of 1,2-diol-type radicals (see refs. 8 and 9 and refs. therein). Radicals obtained by attack at all C-H positions can be recognised

**Table 2** EPR Parameters for radicals produced by HO $\cdot$  attack [generated from the reaction of Fe(II)-oxalate with H<sub>2</sub>O<sub>2</sub> or Ti(III) with H<sub>2</sub>O<sub>2</sub>] on some models of carbohydrates

Substrate	Radical	Hyperfine splittings/mT $\pm$ 0.01			<i>g</i> -value $\pm$ 0.0001
		<i>a</i> ( $\alpha$ -H)	<i>a</i> ( $\beta$ -H)	<i>a</i> (other)	
Diethyl ether	$\cdot\text{CH}_2\text{CH}_2\text{OEt}$ (1)	2.22 (2 H)	2.77 (2 H)	—	2.0027
	$\cdot\text{CHMeOEt}$ (2)	1.42 (1 H)	2.16 (3 H)	0.137 (2 H)	2.0031
		1.23 (1 H)	2.84 (2 H)	0.16 (2 H) 0.08 (2 H)	2.0031
THF		2.13 (1 H)	3.51 (4 H)	—	2.0026
					
Propane-1,2-diol	$\cdot\text{CH}(\text{OH})\text{CHMeOH}$ (5)	1.75 (1 H)	1.235 (1 H)	0.06 (3 H) 0.06 (OH)	2.0031
	$\cdot\text{CMe}(\text{OH})\text{CH}_2\text{OH}$ (6)	—	2.10 (3 H) 0.915 (2 H)	—	2.0031
	$\cdot\text{CH}_2\text{CH}(\text{OH})\text{CH}_2\text{OH}$ (7)	2.21 (2 H)	2.44 (1 H)	—	2.0027
Tetrahydrofurfuryl alcohol		2.13 (1 H)	3.40 (2 H) 3.73 (2 H)	—	2.0027
		2.13 (1 H)	3.43 (2 H) 2.72 (1 H)	—	2.0026
		1.86 (1 H)	0.93 (1 H)	—	2.0031
		1.25 (1 H)	2.57 (1 H) 2.15 (1 H)	0.2 (1 H) 0.07 (2 H)	2.0031

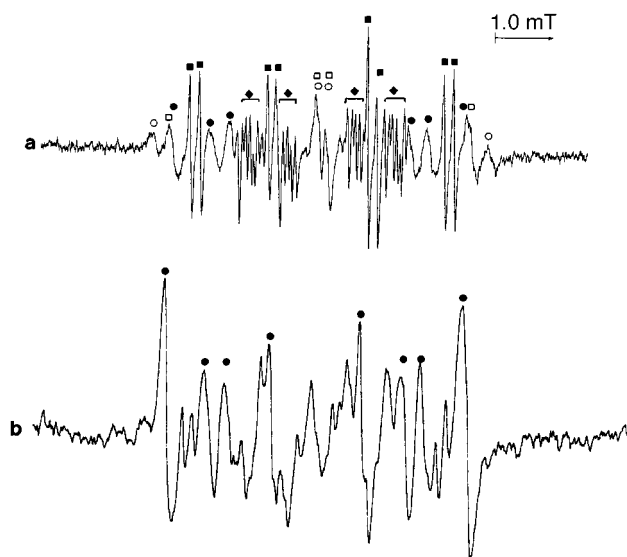
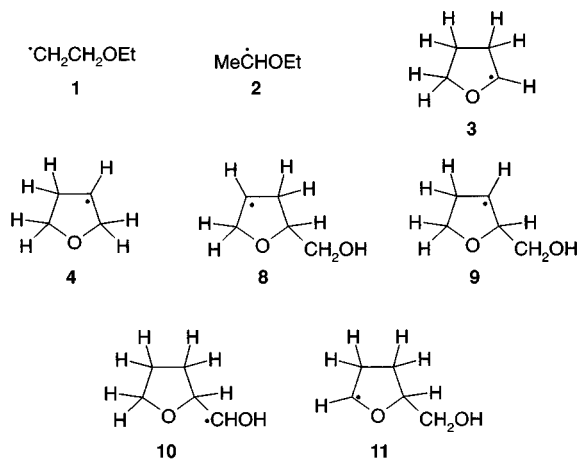
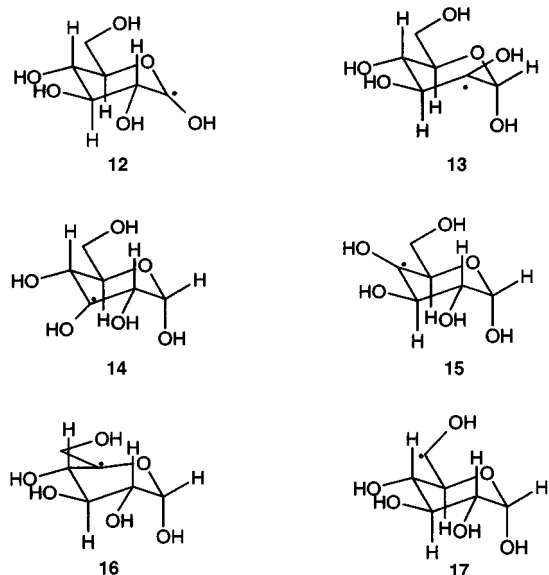


Fig. 3 EPR spectra of radicals (**13**, ■), (**14**, ○), (**15**, □), (**16**, ●) and (**17**, ◆) obtained from the reaction of  $\alpha$ -D-glucose (50 mM), hydrogen peroxide (8 mM) and a solution of (a) Ti(III)-EDTA (2 mM); (b) Fe(II)-oxalate (2 mM).



from their hyperfine splittings; their structural assignments (to **12**–**17**) and rationale will not be repeated here.

Fig. 3(b) illustrates the spectrum obtained in the corresponding Fe(II)-oxalate/ $H_2O_2$  experiment. The lines are some-



what broader than in the Ti(III)/ $H_2O_2$  experiment as a result of the paramagnetic broadening induced by the presence of Fe(II) and Fe(III), although this does allow use of a higher modulation amplitude (and hence enhancement of signal-to-noise ratio). The hyperfine splittings [essentially identical to those obtained previously using the Ti(III)/ $H_2O_2$  couple, as expected] are given in Table 2. Several features are of note. Firstly, despite the lack of resolution, signals from all but one of the individual radicals (obtained by C–H abstraction) can be recognized: this strongly suggests, as we have claimed here and previously, that the reactive entity is the hydroxyl radical (with perturbation in steady-state concentrations reflecting the occurrence of *secondary* reactions). Secondly, there are no detectable signals from the C<sup>1</sup> radical **12**, which is perhaps not surprising given the *two*  $\alpha$ -oxygen substituents and the expectation that this will enhance the ease of oxidation. Thirdly, the dominant radical is **16**, from C<sup>5</sup>, with the radicals from C<sup>2</sup> **13** and C<sup>6</sup> **17** also prominent; there are traces of signals from abstraction from C<sup>3</sup> and C<sup>4</sup> (**14** and **15**, respectively). This pattern can be understood if the rate constants for oxidation [by Fe(III)] of the first-formed radicals are in the order: C<sup>5</sup> < C<sup>2</sup> ~ C<sup>6</sup> < C<sup>3</sup> ~ C<sup>4</sup> < C<sup>1</sup>. Given the complexity of the system, individual rate constants cannot be estimated reliably.

The relative ease of oxidation of the C<sup>3</sup> and C<sup>4</sup> radicals again reflects the presence of the  $\alpha$ -OH substituent (*cf.* related ethanol- and diethyl ether-derived radicals). The retardation of oxidation of species with the radical centre at C<sup>2</sup>, C<sup>6</sup> and C<sup>5</sup> is believed to reflect a lowering of the rate constant for oxidation owing to the presence of a  $\beta$ -oxygen substituent in which significant electronic overlap occurs between the orbital of the unpaired electron and an *eclipsing*  $\beta$ -C–O bond. This interaction, which has been reported before for the radical  $\cdot CH(OH)CH_2OH$  and related species,<sup>11</sup> causes eclipsing between the singly-occupied orbital and the  $\beta$ -C–O bond, resulting in a locked conformation (see **18**) and very low  $\beta$ -proton splittings; this also results in reduced electron-rich character at C<sub>u</sub> and hence a decrease in the rate of oxidation. Similar interactions are revealed by the low  $a(\beta-H)$  values for the radicals from C<sup>5</sup>, C<sup>6</sup> (see **19** and **20** for preferred conformations) and C<sup>2</sup> for which the eclipsing nature of the C<sup>1</sup>–OR bond is dictated by the stereochemistry of the  $\alpha$ -D-glucose isomer, an example of the anomeric effect. Similar trends have been observed for the relative rate constants for addition of radicals **13**, **16** and **17** to  $CH_2=CMeCO_2H$ .<sup>12</sup>

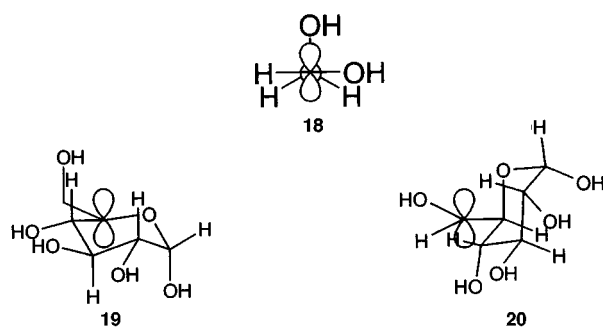


Fig. 4 shows the spectrum obtained from  $\beta$ -D-glucose under similar conditions. Again, the spectrum shows a mixture of radicals which can be assigned on the basis of the well-resolved spectra obtained from Ti(III)/ $H_2O_2$  (for which hyperfine splittings for **21**–**26** have been reported).<sup>9</sup> The dominant signal is again from the C<sup>5</sup>-derived radical **25** for which the extra clarity allows the unambiguous redetermination of the individual  $\beta$ -hyperfine splittings for this species (again, the evidence for restricted rotation from the non-equivalent  $\beta$ -proton splittings is notable): there are also traces of signals from the C<sup>2</sup> **22** and C<sup>6</sup> **26** radicals [together with C<sup>3</sup> **23** and/or C<sup>4</sup> **24** (see Table 3)]. Again, we conclude that  $\cdot OH$  is first formed, that this attacks

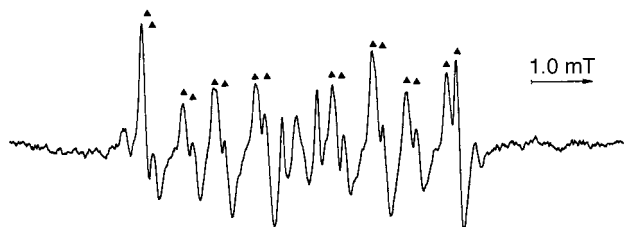


Fig. 4 EPR spectrum of radical (25, ▲) obtained as the dominant radical in the reaction of  $\beta$ -D-glucose (50 mM) with hydrogen peroxide (8 mM) and Fe(II)-oxalate (2 mM).

the carbohydrate more or less randomly and that this is followed by a further oxidation reaction which is slower for the C<sup>5</sup>-derived species; we note that the hyperfine splittings for C<sup>5</sup>- and C<sup>6</sup>-derived radicals (25 and 26, respectively) indicate a beta-eclipsing geometry.

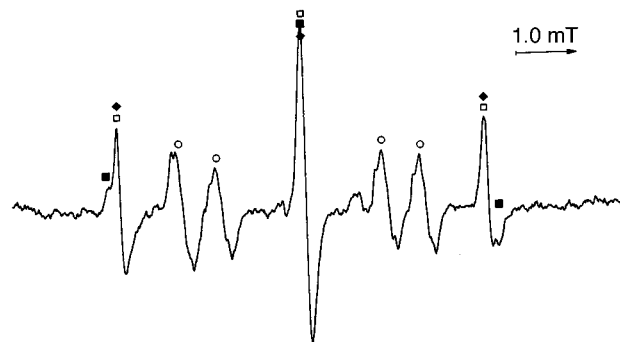
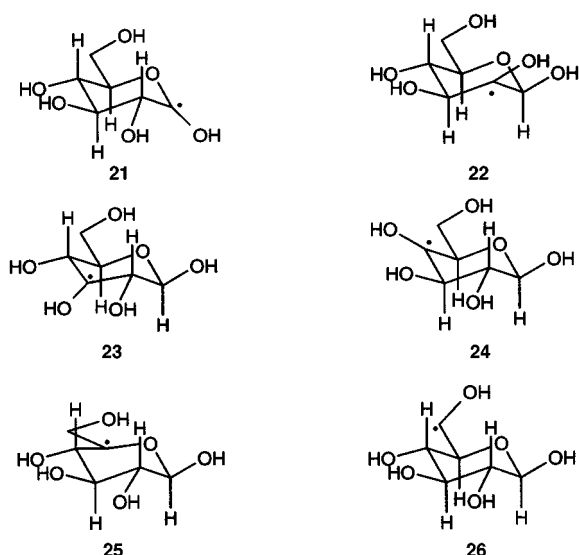


Fig. 5 EPR spectrum of radicals (27, ◆), (28 and 32, ○), (29 and 31, □) and (30, ■) obtained for the reaction of *myo*-inositol (50 mM) with hydrogen peroxide (8 mM) and Fe(II)-oxalate (2 mM).

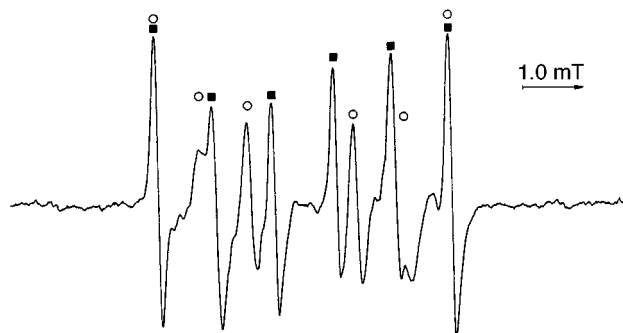
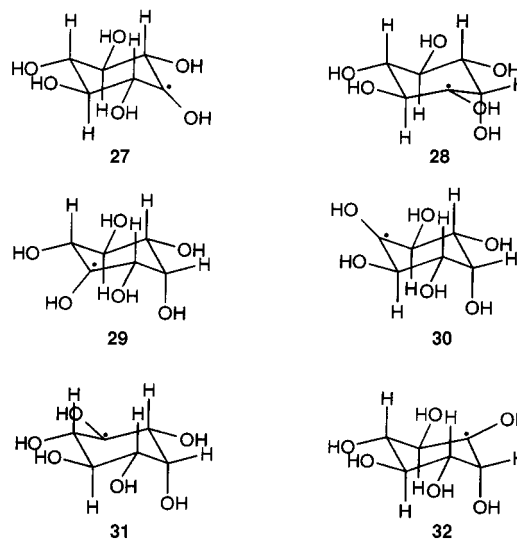


Fig. 6 EPR spectrum dominated by signals for (33, ○) and (34, ■) for the reaction of sucrose (50 mM) with hydrogen peroxide (8 mM) and Fe(II)-oxalate (2 mM).



### 3.2 Reaction of Fe(II)-oxalate/H<sub>2</sub>O<sub>2</sub> with other carbohydrates.

*a) myo-Inositol.* Inspection of the EPR spectra obtained from reaction of *myo*-inositol (0.03 mol dm<sup>-3</sup>) under standard conditions (Fig. 5) indicates that free-radical oxidation has occurred to give hydrogen abstraction from C-H bonds at each ring-position. Assignments to radicals 27–32 are based on results previously reported for the Ti(III)/H<sub>2</sub>O<sub>2</sub> system<sup>8</sup> and given in Table 3: compared with the titanium system, the Fe(II)-oxalate reaction gives slightly broader spectra (so that the smallest hyperfine splittings are not completely resolved). The similarity in behaviour is again striking: one notable difference, however, is the somewhat lower relative concentration of the radicals 27 and 29–31, in which both  $\beta$ -OH groups are equatorial. This is again understandable if the radicals with  $\beta$ -OH groups axial (28 and 32) (and hence more nearly eclipsing) are more resistant to oxidation by Fe(III) (see above).

*b) Sucrose.* The spectra from sucrose and Fe(II)-oxalate/H<sub>2</sub>O<sub>2</sub> (Fig. 6) clearly show signals from a mixture of carbon-centred radicals suggesting the occurrence of attack at a number of sites (*cf.* results from the Ti(III)/H<sub>2</sub>O<sub>2</sub> system).<sup>10</sup> Particularly notable are the dominant signals from 33 and 34 *i.e.* the C<sup>5</sup>-radicals in both the 6- and 5-membered rings. Hyperfine splittings are given in Table 4: individual assignments to the 5- and 6-membered rings are made on the basis of results for  $\alpha$ -D-glucose (see above) and the C<sup>5</sup>-radical from  $\beta$ -fructofuranose.<sup>13</sup> We have previously noted<sup>10</sup> the apparent preference for HO<sup>•</sup> attack at the C<sup>5</sup> position in the 5-membered ring, a selectivity which is believed to reflect the extra stability in the associated transition-state *via* enhanced overlap between the lone-pair in the p-orbital on the ring-oxygen and that on the

incipient radical centre [*cf.* stereoelectronic effects in the reaction of 'BuO<sup>•</sup> with some cyclic and acyclic ethers<sup>14</sup>]; this may well play a part in this case. Additionally, we also conclude that oxidation of radicals of this type is, to some extent, retarded compared to other ring C <sub>$\alpha$</sub> -OH positions, an effect which we again attribute to the eclipsing (stabilising) nature of the  $\beta$ -OH bond in each case. The low  $\beta$ -proton couplings for these radicals are again notable and confirm the strong preference for an eclipsing geometry.

*c)  $\beta$ -D-Cellobiose and D-maltose.* The analysis of the spectra obtained from Fe(II)-oxalate and H<sub>2</sub>O<sub>2</sub> and these substrates is based in part on the relevant spectra obtained with Ti(III) and H<sub>2</sub>O<sub>2</sub> and on the analyses presented above for the related ring systems<sup>9,10</sup> (see Table 4 for hyperfine splittings).

For  $\beta$ -D-cellobiose [two  $\beta$ -glucose units, linked 1,4 (35)] two C<sup>5</sup>-derived radicals, 36 and 37, again dominate the spectrum, as

**Table 3** EPR Parameters for radicals produced by HO<sup>•</sup> attack [generated from the reaction of Fe(II)-oxalate with H<sub>2</sub>O<sub>2</sub>] on some monomeric sugars

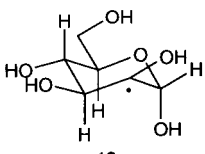
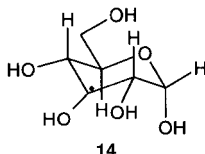
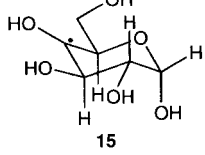
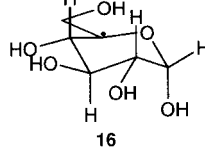
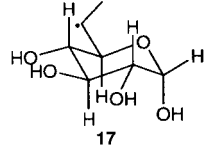
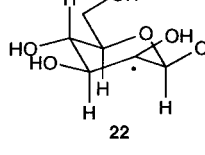
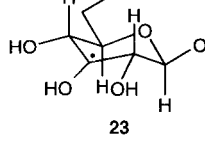
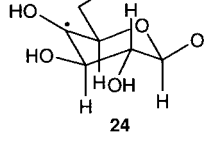
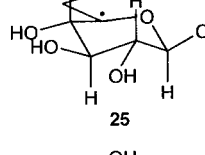
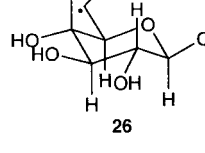
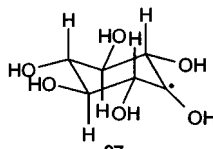
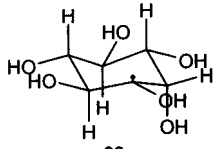
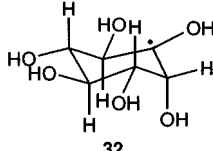
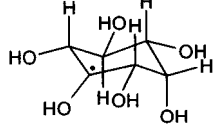
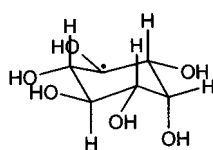
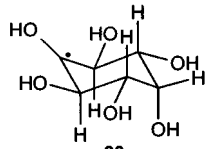
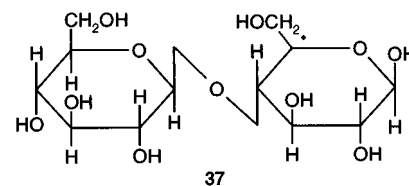
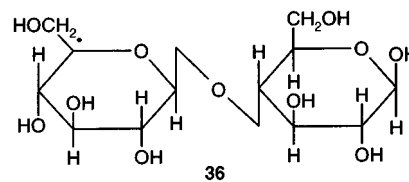
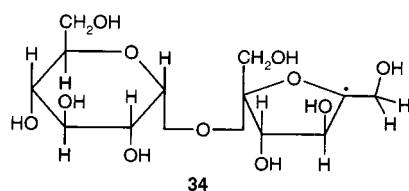
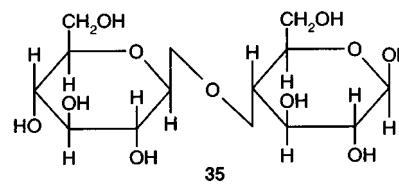
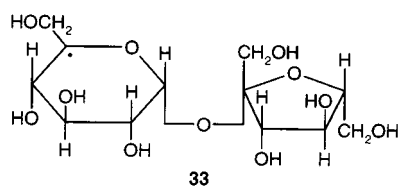
Sugar	Radical	Hyperfine splittings/mT ±0.01			g-value ±0.0001
		a(α-H)	a(β-H)	a(other)	
α-D-Glucose	 13	—	2.97 (1 H) 1.31 (1 H)	—	2.0031
	 14	—	2.93 (1 H) 2.76 (1 H)	—	2.0031
	 15	—	2.46 (1 H) 2.60 (1 H)	—	2.0031
	 16	—	3.33 (1 H) 0.69 (1 H) 0.99 (1 H)	—	2.0031
	 17	1.84 (1 H)	0.62 (1 H)	—	2.0032
β-D-Glucose	 22	—	2.86 (1 H) 2.28 (1 H)	—	2.0031
	 23	—	2.93 (1 H) 2.81 (1 H)	—	2.0031
	 24	—	2.39 (1 H) 2.34 (1 H)	—	2.0031
	 25	—	3.15 (1 H) 1.20 (1 H) 0.64 (1 H)	0.1 (1 H)	2.0031
	 26	1.84 (1 H)	0.75 (1 H)	—	2.0032

Table 3 (Contd.)

Sugar	Radical	Hyperfine splittings/mT $\pm 0.01$			g-value $\pm 0.0001$
		$a(\alpha\text{-H})$	$a(\beta\text{-H})$	$a(\text{other})$	
<i>myo</i> -Inositol			3.00 (2 H)	0.06 (2 H)	2.0031
			3.31 (1 H) 0.63 (1 H)	0.12 (2 H)	2.0031
					
			3.02 (1 H) 2.98 (1 H)	0.04 (1 H)	2.0031
					
			3.16 (2 H)	0.03 (3 H)	2.0031



noted above for sucrose [these have one large  $\beta\text{-H}$  splitting from the adjacent axial proton, two smaller splittings ( $\text{CH}_2\text{OH}$ ) and one low  $\gamma\text{-H}$  splitting typical of the  $\text{C}^5$  radical in  $\beta\text{-glucose}$ ]. Much weaker signals from other radicals could also be detected. We believe that the selectivity observed again reflects retardation of oxidation of the  $\text{C}^5$  species compared with other oxygen-conjugated radicals.

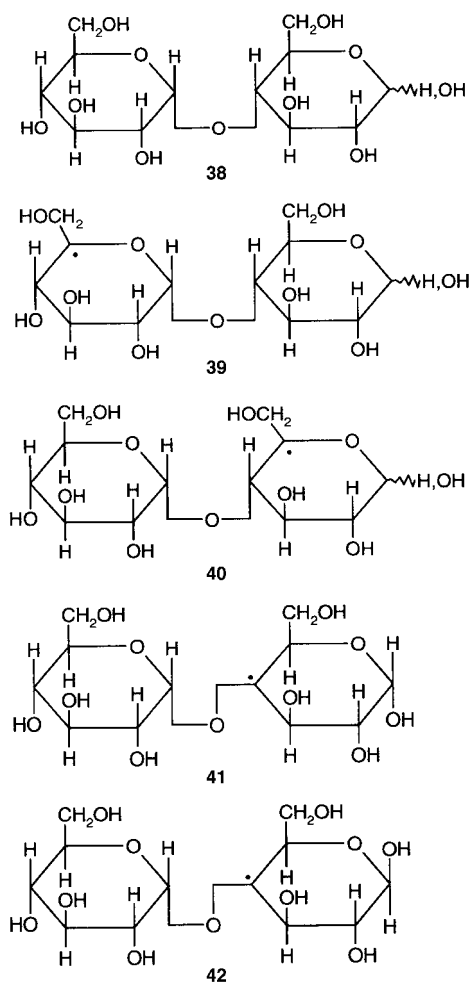
For *D*-maltose [which contains an  $\alpha\text{-glucose}$  unit, linked 1,4 to a second glucose moiety, for which both  $\alpha\text{-}$  and  $\beta\text{-}$  configurations occur (38)] the dominant  $\text{C}^5$  radicals 39 and

40 are clearly identified: an extra, strong signal with two axial  $\beta\text{-}$  protons, characterizes  $\text{C}^3$  and/or  $\text{C}^4$ -centred species. We suggest that these are the two  $\text{C}^4$ -centred species 41 and 42 for which the conformation/geometry is such that, for steric reasons, further oxidation by  $\text{Fe(III)}$  is retarded.

**Table 4** EPR Parameters for radicals produced by HO<sup>•</sup> reaction [generated from the reaction of Fe(II)-oxalate with H<sub>2</sub>O<sub>2</sub>] with some disaccharides

Sugar	Radical <sup>a</sup>	Hyperfine splittings/mT ±0.01		
		<i>a</i> (α-H)	<i>a</i> (β-H)	<i>a</i> (other)
Sucrose	33	3.23 (1 H)	0.88 (1 H) <sup>b</sup> 0.69 (1 H) <sup>b</sup>	—
	34	2.91 (1 H)	0.95 (2 H) <sup>c</sup>	—
β-D-Cellobiose	36	3.81 (1 H)	1.04 (1 H)	0.11 (1 H)
	37	2.99 (1 H)	1.15 (1 H)	0.77 (1 H)
D-Maltose	39 and/or 40 <sup>d</sup>	3.33 (1 H)	1.01 (1 H)	0.67 (1 H)
	41 and/or 42 <sup>d</sup>	2.75 (1 H)	2.35 (1 H)	—

<sup>a</sup> Major species detected. All have *g* 2.0031 ± 0.0001. <sup>b</sup> ±0.05 mT. <sup>c</sup> Non-equivalent splittings not separately measured. <sup>d</sup> Individual assignments not possible.



## Summary

Our EPR experiments, especially when considered together with our earlier findings for the Ti(III)/H<sub>2</sub>O<sub>2</sub>, Fe(II)-EDTA/

H<sub>2</sub>O<sub>2</sub>, and Fe(II)-oxalate/H<sub>2</sub>O<sub>2</sub> systems<sup>4,7</sup> confirm a generality of behaviour which can be interpreted in terms of the following principles: Firstly, the hydroxyl radical is indeed generated in these metal-peroxide (Fenton-type) systems. Secondly, <sup>•</sup>OH reacts *relatively* unselectively with C-H bonds in carbohydrates and model systems (but note that attack at C-H bonds next to oxygen is favoured: *cf.* the α:β ratio for <sup>•</sup>OH and EtOH). Thirdly, the main differences between Ti- and Fe-containing systems reflect the ease of oxidation of oxygen-conjugated radicals by Fe(III) (whether complexed to EDTA or oxalate: the rate constants for this process approach 10<sup>9</sup> dm<sup>3</sup> mol<sup>-1</sup> s<sup>-1</sup>). Fourthly, an eclipsing β-oxygen substituent (as in most of the C<sup>5</sup>- and C<sup>6</sup>-radicals derived from the sugars reported, and as revealed by the low β-proton coupling constants) significantly reduces the rate of oxidation by Fe(III).

The rapid oxidation of most of the oxygen-conjugated radicals will have several important consequences. Firstly, reduction of Fe(III) regenerates more Fe(II) which of course reacts rapidly with H<sub>2</sub>O<sub>2</sub> (a classic, catalytic Fenton oxidation system). Secondly, the reaction of the incipient carbonium ion obtained will lead to either a carbonyl group (*via* deprotonation) or, for ring junctions, hemiacetal or orthoester formation. The first of these gives an oxidized substrate susceptible to further radical attack;<sup>15</sup> the others, *via* hydrolysis, lead to polysaccharide degradation.<sup>16</sup> For disaccharides, it is also notable that initial <sup>•</sup>OH attack appears to be favoured to some extent at the C<sup>5</sup> position, adjacent to the ring-oxygen, a reaction which provides an extra opportunity for cleavage, *via* fission of the O-C<sup>1</sup> bond.<sup>16,17</sup>

It should also be noted that carboxyl groups (in addition to those present naturally in cellulose)<sup>18</sup> will result from free-radical oxidation of the C<sup>1</sup>-hemiacetal at the “reducing” terminus of a cellulose chain. We believe that these groups will be a locus for further complexation of Fe(III). With iron thus bound, and H<sub>2</sub>O<sub>2</sub> (and oxalate) relatively mobile, this provides a mechanism for multiple production of <sup>•</sup>OH at the same site, which may well explain, on a molecular level, the cleavage of cellulose into microcrystallites by brown rot fungi.

The experiments reported here have been carried out in anaerobic conditions—in part, to prevent EPR line-broadening and complications from peroxy radical chemistry. Under oxygenated conditions, carbon-centred radicals will react rapidly with oxygen to give peroxy radicals, which are known to undergo a variety of further fragmentation reactions which serve to amplify the damage described above.<sup>16</sup>

## Experimental

EPR Spectra were recorded on a Bruker ESP-300 spectrometer equipped with an X-band klystron and 100 kHz modulation. Typical conditions were centre field 348.5 mT; sweep width 10 mT; frequency 9.77 GHz; power 20 mW; scan time 670 s; time constant 670 ms; modulation amplitude 0.1 mT. All chemicals were purchased from the Sigma/Aldrich Company. Deionised water was used for all experiments. FeSO<sub>4</sub>·7H<sub>2</sub>O was used as the source of Fe(II). Solutions of oxalate were prepared from stock solutions of oxalic acid and dipotassium oxalate. Ti(III)Cl<sub>3</sub> (>10 wt.% solution in HCl) was used as the source of Ti(III). Na<sub>2</sub>-EDTA was used when EDTA was added as a complexing agent.

The continuous flow apparatus employed a three-way mixing system as described previously.<sup>7</sup> The flow rate, typically 40 cm<sup>3</sup> s<sup>-1</sup> was maintained with a Watson-Marlow 502s peristaltic pump, positioned on the inlet tubes. The delay time between mixing and passage through the EPR cavity was *ca.* 30 ms. All solutions were deoxygenated both prior and during use by purging with oxygen-free nitrogen. Final adjustment of pH was made by addition of conc. ammonia or conc. sulfuric acid solutions to the metal-ion stream. All experiments were carried out at pH 4. Typical concentrations after mixing were: stream 1,



Fe(II) 2.0 mM and oxalate 10 mM; stream 2, H<sub>2</sub>O<sub>2</sub> 8 mM; stream 3, substrate 30 mM. Relative radical concentrations were determined by double-integration; absolute radical concentrations were estimated by comparison with signals obtained from Ti<sup>III</sup>/H<sub>2</sub>O<sub>2</sub>/EtOH under standard conditions.<sup>7</sup>

Kinetic simulations were performed using a program originally written by Dr T. M. F. Salmon and modified to run on an IBM-PC clone.

### Acknowledgements

We thank the BBSRC for funding (J. S. B. P.) and EPSRC for provision of instrumentation.

### References

- 1 K.-E. L. Eriksson, R. A. Blanchette and P. Ander, *Microbial and enzymatic degradation of wood and wood components*, Springer, Berlin, 1990.
- 2 S. M. Hyde and P. M. Wood, *Microbiology*, 1997, **143**, 259.
- 3 F. Green, M. J. Larsen, J. E. Winandy and T. L. Highley, *Mater. Org.*, 1991, **26**, 191.
- 4 J. S. B. Park, P. M. Wood, M. J. Davies, B. C. Gilbert and A. C. Whitwood, *Free Rad. Res.*, 1997, **27**, 447.
- 5 T. K. Kirk, R. Ibach, M. D. Mozuch, A. H. Conner and T. L. Highley, *Holzforschung*, 1991, **45**, 239.
- 6 B. C. Gilbert, R. O. C. Norman, P. S. Williams and J. N. Winter, *J. Chem. Soc., Perkin Trans. 2*, 1982, 1439.
- 7 S. Croft, B. C. Gilbert, J. R. Lindsay Smith and A. C. Whitwood, *Free Rad. Res. Commun.*, 1992, **17**, 21.
- 8 B. C. Gilbert, D. M. King and C. B. Thomas, *J. Chem. Soc., Perkin Trans. 2*, 1980, 1821.
- 9 B. C. Gilbert, D. M. King and C. B. Thomas, *J. Chem. Soc., Perkin Trans. 2*, 1981, 1186.
- 10 B. C. Gilbert, D. M. King and C. B. Thomas, *J. Chem. Soc., Perkin Trans. 2*, 1983, 675.
- 11 A. J. Dobbs, B. C. Gilbert and R. O. C. Norman, *J. Chem. Soc., Perkin Trans. 2*, 1972, 786.
- 12 B. C. Gilbert, J. R. Lindsay Smith, S. R. Ward, A. C. Whitwood and P. Taylor, *J. Chem. Soc., Perkin Trans. 2*, 1998, 1565.
- 13 M. Fitchett, B. C. Gilbert and M. Jeff, *Philos. Trans. R. Soc. London B*, 1985, **311**, 517.
- 14 V. Malatesta and K. U. Ingold, *J. Am. Chem. Soc.*, 1981, **103**, 609.
- 15 R. O. C. Norman and R. J. Pritchett, *J. Chem. Soc. B*, 1967, 378.
- 16 C. von Sonntag, *Adv. Carbohydr. Chem. Biochem.*, 1980, **37**, 7.
- 17 See e.g. M. N. Lehmann, M. G. Bakker, H. Patel, M. L. Partin and S. J. Dormady, *J. Inclusion Phenom. Mol. Recognit. in Chem.*, 1995, **23**, 99; M. J. Perkins and B. P. Roberts, *J. Chem. Soc., Perkin Trans. 2*, 1975, 77.
- 18 E. Schmidt, W. Jandebaur, M. Hecker, R. Schnegg, M. Atterer, W. Hahn and J. W. Pedlow, *Ber. Dtsch. Chem. Ges. B*, 1936, **69**, 366; K. Szakmary, A. Wotawa and C. P. Kubicek, *J. Gen. Microbiol.*, 1991, **137**, 2873.

Paper 9/00882I